Original Article

Urtica dioica Mediates Zinc-Copper Doped Nanoparticles as Potent Anticancer Agents against Human Breast Cancer MDA-MB-231 Cell Line

Fatemeh Tavanaei, Azadeh Mohammadgholi, Nastaran Asghari Moghaddam
Department of Biology, Central Tehran Branch, Islamic Azad University, Tehran, Iran

Abstract

Background: Recently, biosynthesis, also recognized as green synthesis, has emerged as an alternative for producing nano-metal oxides. In this study the anti-cancer activity of green-synthesized zinc-copper-doped *NPs* using *Urtica dioica* against the human BC-MDA-MB-231 cell line was investigated.

Materials and Methods: The synthesized bimetallic NPs using *U. dioica* through Fourier transform infrared spectroscopy (FTIR), X-ray diffraction (XRD), dynamic light scattering (DLS), transmission electron microscopy (TEM), and scanning electron microscopy (SEM), coupled with energy-dispersive analysis of X-rays (EDX) and UV-Visible spectroscopy was characterized. MTT assay assessed the toxicity in BC cells induced by *NP* exposure, determining the lethal toxic dose. Additionally, apoptosis in cells resulting from NP exposure was evaluated using the real-time PCR technique. The potential mechanism of toxicity induced by doped NPs was further assessed by lactate dehydrogenase, caspase-3, and ROS generation in BC cells.

Results: The particles exhibited an irregular structure with non-uniform surfaces, and a variable size of NPs ranging between 22 and 46 nm was observed. Zn-doped-Cu NPs decreased the viability of MDA-MB-231 cells in both treatment groups in a dose-dependent manner. The IC_{50} concentration of Zn-doped-Cu NPs significantly increased *Bax* expression and decreased *Bcl2*, *MMP2*, and *MMP9* genes thus playing a crucial role in apoptosis and metastasis prevention. Furthermore, a notable increase in LDH activity, caspase-3 activity, and ROS generation was observed in cancerous cells following exposure to biosynthesized NPs compared to MDA-MB-231 cells receiving extract and the control group.

Conclusions: These findings underscore the remarkable apoptotic, antimetastatic, and antioxidant activity of biosynthesized Zn-doped-Cu NPs.

Keywords: Apoptosis, biosynthesis, breast cancer, MDA-MB-231, nanoparticles

Address for correspondence: Dr. Azadeh Mohammadgholi, Department of Biology, Central Tehran Branch, Islamic Azad University, Tehran, Iran.
E-mail: a.mohammadgholi@yahoo.com

Submitted: 14-Dec-2023; **Revised:** 17-Mar-2024; **Accepted:** 02-Apr-2024; **Published:** 30-Apr-2025

Introduction

Breast cancer (*BC*) is a prevalent malignancy among women, ranking as the most frequent cancer worldwide in this population.[1] Treatment modalities, such as surgery, radiation, or systemic therapy, are tailored to the specific biological subtype and cancer stage.[2] Chemotherapy remains a crucial therapeutic option for several subtypes of *BC* characterized by poor treatment outcomes due to their high metastatic potential and lack of established therapeutic targets.[3] Addressing drug resistance necessitates adopting innovative, customized approaches.[4] Nanomedicine-based techniques have garnered significant interest in cancer treatment owing to the targeted delivery, biocompatibility, high absorption, and multifunctionality of *NPs*.[3]

Ionic zinc plays pivotal roles in immune function, homeostasis, oxidative stress responses, apoptosis, and aging processes within

Access this article online

Quick Response Code:

Website: https://journals.lww.com/ADBM

DOI: 10.4103/abr.abr_515_23

How to cite this article: Tavanaei F, Mohammadgholi A, Asghari Moghaddam N. *Urtica dioica* mediates zinc-copper doped nanoparticles as potent anticancer agents against human breast cancer MDA-MB-231 cell line. Adv Biomed Res 2025;14:30.

regular biological cycles.[5] Its chemical treatment application in cancer is desirable due to its ability to reduce cellular metabolism, modulate gene expression, and induce apoptosis in cancerous cells.[6,7] *ZnONP*s exhibit enhanced selectivity for cancer cells and exert more significant cytotoxicity against BC than normal cells.[4] Unlike conventional chemotherapeutic agents, *ZnONPs* offer therapeutic doses with heightened cancer cell selectivity.[8]

Irrespective of production methods, *ZnONPs* find applications in diverse fields, such as inhibition of antidiabetic activity,[9] antimicrobial action,[10] anti-inflammatory effects,[11] wound healing,[12] cancer diagnosis and imaging,[13] and anti-tumor activity.[14] Similarly, copper nanoparticles (*Cu-NP*) have been extensively studied for their antibacterial properties, with recent reports suggesting antiviral and anti-cancer potentials. The combination of green-synthesized zinc and copper *NPs* demonstrates synergistic toxicity against lung and human melanoma cell lines when compared to *Cu-NP* or *Ag-NP* alone.[15] Evidence suggests that *Zn*-doped-*Cu NPs* could be potent anti-cancer agents for MCF-7 BC.[15]

Biosynthesis, or *green synthesis*, emerges as an alternative method for producing nano-metal oxides.[16] *Urtica dioica*, a perennial plant from the *Urticaceae* family, has historically been used to treat cardiovascular diseases, particularly hypertension.[17] Studies indicate that extracts from *U. dioica* possess antioxidant, mutagenic, and proliferative properties.[18] Investigation into compounds derived from *U. dioica* and *Urtica parviflora* demonstrates significant anti-cancer activity against the MDA-MB-231 cell line.[19] Additionally, extracts from *Nettle* and *Clove* exhibit inhibitory effects on BC cell proliferation.[20] Furthermore, studies by Karakol P. *et al*.[21] or Nafeh G. *et al*.[22] indicate that *U. dioica* induces higher *caspase 3*, *p53*protein, and TUNEL-positive cells in human BC cells than untreated cells.

Biological synthesis techniques are employed to produce Zn-doped-Cu NPs to mitigate adverse environmental impacts. This approach offers several advantages, including producing safe *NPs* with minimal harmful byproducts, biocompatibility, cost-effectiveness, scalability, and immunogenicity.[23]

Numerous investigations have explored the potential of *NPs* in cancer therapy. For instance, Bangroo A. *et al*.[24] demonstrated decreased viability of MDA-MB-231 BC cells when treated with *Catharanthus roseus* leaf extract combined with zinc oxide nanoparticles (*ZnO NPs*). Darvish M. *et al*.[25] synthesized $CuFe_2O_4$ *NPs* doped with *Zn* using nasturtium extract, resulting in enhanced cytotoxic effects against A549 cancer cells compared to $CuFe_2O_4$ *NPs* alone. Mahmood RI *et al*.[26] also revealed that copper oxide nanoparticles (*CuO NPs*) synthesized with *Annona muricata L* plant extract induce apoptosis in AMJ-13 and MCF-7 BC cell lines. *Zn*-CuO *NPs* synthesized by VD1142 exhibit potent anti-cancer proliferation activity, as demonstrated by Zhang H. *et al*.[27]

This study aims to synthesize Zn-doped-Cu NPs utilizing *U. dioica* as a cancer-fighting agent and evaluate their cytotoxicity in MDA-MB-231 BC cells.

Various characterization techniques, including transmission electron microscopy (*TEM*), X-ray diffraction (*XRD*), scanning electron microscopy (*SEM*), Fourier transform infrared spectroscopy (*FTIR*), dynamic light scattering (*DLS*), energy dispersive analysis of X-rays (*EDX*), and UV-visible spectroscopy are employed. Toxicity induced by NP exposure in BC cells is assessed through the MTT test to determine the lethal dosage, while real-time PCR is utilized to examine NP-induced apoptosis. Additionally, the generation of lactate dehydrogenase, caspase 3, and ROS in BC cells aids in assessing the potential mechanism of toxicity caused by doped NPs.

Materials and Methods

Materials

Fetal bovine serum (*FBS*), 3-(4,5-dimethylthiazol-2-yl)-2,5-diphenyltetrazolium bromide (*MTT*), medium *RPMI-1640*, penicillin/streptomycin 100×, phosphate-buffered saline (*PBS*), trypsin-EDTA, and trypan blue were acquired from Gibco (*ThermoFisher Scientific, USA*). $AgNO_3$ and $Zn(NO_3)_2{\cdot}6H_2O$ were purchased from Merck (*Germany*). The dried leaves of *U. dioica* were obtained from the *Iranian Biological Resource Center*. The *MDA-MB-231* cell lines were procured from the *Cell Bank of Pasteur Institute (Iran)*. The *RNA Qiagen* extraction kit (*USA*) and the *RevertAid First Strand cDNA Synthesis Kit* (*Lithuania*) were utilized.

Synthesizing and characterization of Zn-doped-Cu NPs using Urtica dioica

The *U. dioica* plant was obtained from the *Iranian Center for Biological Resources'* plant bank, authorized by the *Department of Botany*, and assigned the *IBRC* barium number 1358. Aerial parts of the *U. dioica* plant were initially air-dried and then thoroughly dried in the shade to prepare the extract. The leaves were powdered using an electric grinder and stored in glass containers. The *Soxhlet* technique was employed for powder extraction by mixing 500 cc of an aqueous solvent with 50 g of powdered plant leaves. After a 12-hour extraction period, a rotary evaporator (*Rv10 digital, Germany*) was used to remove the solvent. The resulting extract, prepared from the acquired solid powder and double distilled water (*DW*), was stored at 4°C.[28] Zn-doped-Cu NPs were synthesized by combining 0.1 M copper sulfate ($CuSO_4$) and 1 M zinc sulfate ($ZnSO_4$) in 100 ml of *DW*. Subsequently, 4 - 5 ml of extract was added, and the mixture was agitated overnight. The color change indicated the formation of Zn-doped-Cu NPs. The sediment was washed thrice with *DW* and centrifuged for 20 minutes at 13000 rpm after each wash. The product underwent an additional ethanol wash before being heated at 60°C for two hours. It was then left at 37°C for 4 hours. The crystal phase of the Zn-doped-Cu NPs powders was analyzed using *XRD* (*PW3710, Netherlands*) with CuK radiation (λ = 0.0260 nm), and *Fourier-transform*

infrared (FTIR) spectroscopy was conducted using a *UV-1800UV* spectrophotometer (*Shimadzu, Japan*). *Energy-dispersive spectroscopy (EDS)*, *SEM* (*MIRA3, TE-SCAN, CR*), and transmission electron microscopy (*EM10C-100 KV Zeiss, Germany*) were used to assess particle size, shape, and distribution. The synthesized *NPs* shape, structure, and charge density were analyzed via the *dynamic light scattering (DLS)* technique (*Zetasizer-DLS, Malvern, United Kingdom*).

Cell culture

The cell lines *MDA-MB-231* human BC and *MCF10A* were obtained from the Iranian Pasteur Institute's cell bank. They were cultured in *RPMI 1640* medium (Gibco, US) supplemented with 10% fetal bovine serum (*FBS*) (Gibco, USA), *L*-glutamine (Sigma-Aldrich, Germany), and 1% penicillin-streptomycin (Gibco, USA). Cells were utilized within 20 passages. The culture conditions involved maintenance at 37°C in a humidified atmosphere with 5% CO_2.

In vitro cytotoxicity assay

In vitro, cytotoxicity was evaluated using the MTT method. Briefly, cells were seeded in 96-well plates at a density of 1×10^4 cells/100 µL and treated with varying concentrations of Zn-doped-Cu NPs (3.125, 6.25, 12.5, 25, 50, and 100 µg/mL) after 24 hours of incubation at 37°C. Similarly, various concentrations of *U. dioica* extract (3.125, 6.25, 12.5, 25, 50, and 100 µg/mL) were tested. Cytotoxicity against healthy cells (*MCF10A*) was also assessed. Each well received 100 µL of MTT solution (Sigma-Aldrich, Germany) and was further incubated for 24 hours at 37°C with 5% CO_2 humidity. Triplicate analyses were conducted for both plant extract and Zn-doped-Cu NP concentrations. Cell viability percentage was computed using the formula:

Cell viability (%) = OD of Control−OD of ZnO−NP treatment OD of Control ×100

A dose–response curve was plotted to determine the 50% growth inhibition concentration (IC_{50}).

Gene expression by quantitative real-time PCR

RNA extraction from untreated and treated *MDA-MB-231 cells* with IC50 concentrations of Zn-doped-Cu NPs and *U. dioica* extract was performed using the *RNX-Plus* kit (CinnaGen, Iran) following the manufacturer's instructions. Subsequently, reverse transcription PCR (RT-PCR) was carried out using the *Fermentas Revert Aid*™ First Strand cDNA Synthesis Kit (USA). Quantitative real-time PCR (qRT-PCR) was conducted using the *ABI 7300* system (Applied Biosystems Foster City, USA). A 25 µL pre-mix containing 1 µL of primers, 12.5 µL of SYBR-Green PCR Master Mix (Applied Biosystems, UK), 10.5 µL of RNase-free water, and 1 µL of cDNA was prepared. Primer sequences for target genes are provided in Table 1, obtained from www.ncbi.nlm.nih.gov.

The PCR conditions involved an initial activation step at 95°C for 10 min, followed by 40 cycles of denaturation at 95°C for 15 s and synthesis/annealing at 60°C for 30 s. A dissociation curve was generated post-PCR to validate the results. Gene expression levels (*Bax*, *Bcl2*, *MMP2*, and *MMP9*) were normalized to the reference gene (β-*actin*) using the 2−ΔΔCt method, where 2 represents the amplification efficiency factor.

Table 1: Genes used in quantitative real-time-PCR (qRT-PCR)

Gene	Primer sequence
MMP2	Forward: 5'- F: TTG ACG GTA AGG ACGGAC TC-3'
	Revers: 5'- CAT ACT TCA CAC GGA CCA CTTG -3'
β-actin	Forward: 5'- TCCTCCTGAGCGCAAGTAC-3'
	Revers: 5'- CCTGCTTGCTGATCCACATCT-3'
Bax	Forward: 5'- GAGCTGCAGAGGATGATTGC-3′
	Revers: 5'- AAGTTGCCGTCAGAAAACATG-3'
Bcl2	Forward: 5'- ATTGGGAAGTTTCAAATCAGC-3′
	Revers: 5'- CAGTCTACTTCCTCTGTGATGTTG-3'
MMP9	Forward: 5'- GCACGACGTCTTCCAGTACC -3′
	Revers: 5'- CAGGATGTCATAGGTCACGTAGC -3'

Lactate dehydrogenase (LDH) activity measurement

The LDH activity in *MDA-MB-231* cancer cells treated with extracts and NPs was measured using the commercial LDH-Cell Cytotoxicity Assay Kit from ZELIX company, following the provided instructions. In brief, 2×10^4 cells were cultured in a 96-well microtiter plate and incubated in a CO_2-incubator. Forty-five minutes before commencing the experiment, 10 µL of 10× Cell Lysis Solution was added to each well, including Lysis Control wells, followed by incubation at 37°C in a CO_2 incubator for 45 minutes. Subsequently, the wells underwent centrifugation at 600 g for 10 minutes, and 50 µL of culture supernatant was collected from each well and transferred to a new 96-well transparent flat-bottom plate. A total of 50 µL of LDH Working Solution was then added to the wells, gently mixed for 30 seconds, and incubated at ambient temperature. Next, 50 µL of Stop Solution was added to the wells, followed by gentle mixing. The absorbance signal was read at 490 nm, and background absorbance was measured at 650 nm.

$$\% \text{ Relative cytotoxicity} = 100 \times \frac{OD\ experimental\ sample - OD\ untreated\ cells\ control}{OD\ lysis\ control - OD\ untreated\ cells\ control}$$

Caspase activity measurement

Caspase-3 / 7 activity was assessed using a caspase assessment kit per the manufacturer's instructions (Kiazist, Iran). *MDA-MB-231* cell lines were seeded at 4×10^4 cells/well on a 6-well plate, cultured to 70% confluence, and treated for 48 hours with the IC_{50} concentration of *U. dioica* extract and green-synthesized Zn-doped-Cu NPs. The cells were then extracted and centrifugated for 3 minutes at 1500 rpm. The supernatant was discarded, and each well was treated with cell lysis solution, dithiothreitol (DTT), caspase buffer, and caspase substrate for 2 hours at 37°C. Finally, the absorbance was measured using an ELISA reader at 405 nm. All experiments were conducted in triplicate.

Reactive oxygen species (H2-DCFH-DA) assay

The oxidative stress (ROS) levels generated by the samples were quantified using the 2',7'-dichlorodihydrofluorescein diacetate (DCHF-DA) kit.

The 2',7'DCHF-DA acetyl esters, formed through the reduction of DCHF-DA, emitted fluorescence at 530 nm, indicating oxidative stress. MDA-MB-231 human BC cells were exposed to $IC_{50\ sample}$s for 24 hours, followed by a saline buffer wash and subsequent incubation at 37°C for 30 min with 80 mM H2DCFDA. Fluorescence intensity was measured using a microplate reader.

Statistical analysis

Data analysis was conducted using SPSS version 20.0 and GraphPad Prism version 8.0. One-way analysis of variance (ANOVA) was employed, and significance was determined at $P \leq 0.05$.

Results

Biosynthesis and characterization of Zn-doped-Cu NPs

The SEM test results are depicted in Figure 1AI, revealing an irregular structure with non-uniform surfaces and a variable size of NPs ranging between 22 and 46 nm. The TEM results in Figure 1AII exhibit NPs arranged in multifaceted structures forming agglomerates. The mean size of the particles was measured at 9.72 nm, indicating the appropriate and small size of the prepared NPs. Discrepancies in size between SEM and TEM tests may be attributed to the agglomeration of distinct NPs, which may not be well resolved in the TEM diffraction microscope, resulting in the observation of clustered NPs.[29] Figure 1E displays the EDS test results for Zn-doped-Cu NPs, demonstrating the presence of elements constituting the NPs and confirming that the firm peaks correspond to the existence of the primary elements, *zinc* and *copper* alloy, in the green-synthesized NPs. According to the UV-visible study, an absorption peak is evident at 480 nm [Figure 1D]. Throughout reactions and optimization, no significant peak shifts were observed. Previous research indicates that the UV spectra for CuO NPs ranged from 440 to 480 nm.[30] TEM, SEM, and DLS techniques were employed to evaluate the size and morphology of biosynthesized Zn-doped-Cu NPs [Figure 1AIII]. X-ray diffractometry was utilized to ascertain the XRD spectra of the biosynthesized Zn-doped-Cu NPs, identifying several crystal planes with corresponding XRD values, including (100), (002),

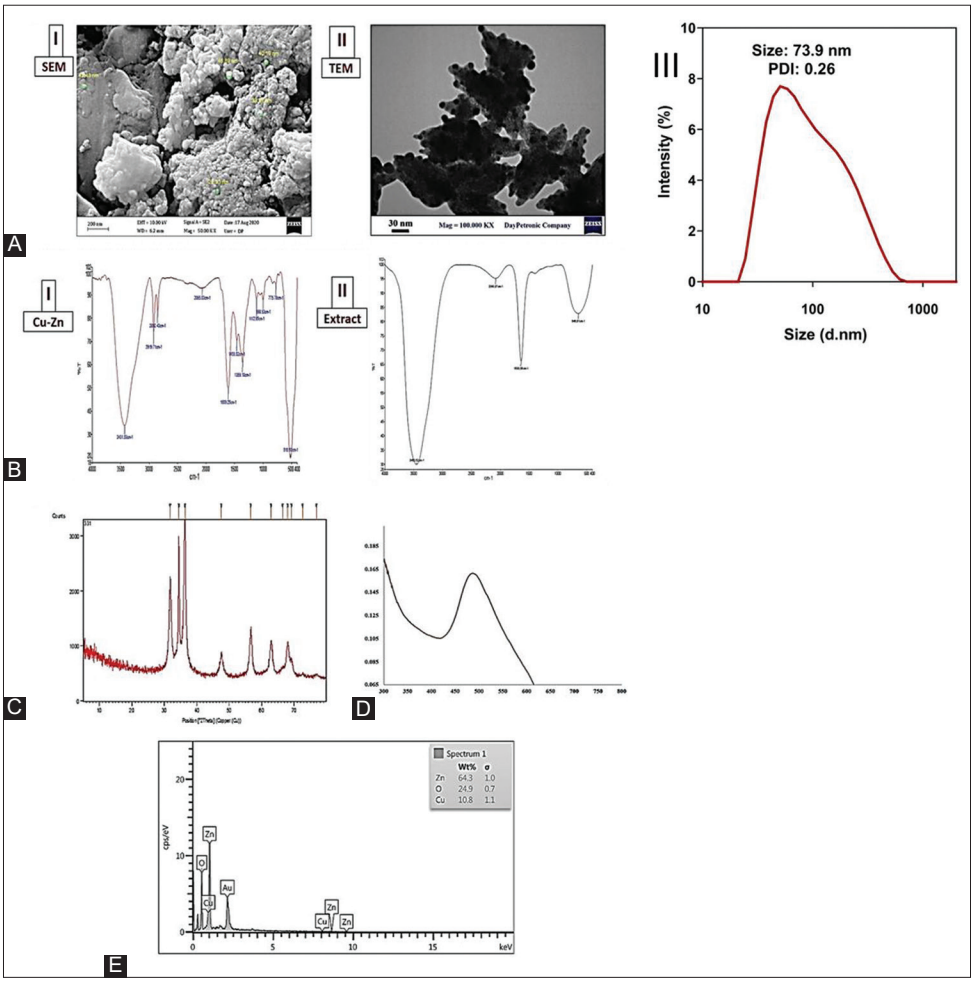

Figure 1: (AI) SEM, (AII) TEM, and DLS graph of biosynthesized Zn-doped-Cu NPs (AIII). The DLS data exhibit NPs with a size of 73.9 nm and PDI = 0.26. FTIR spectra of (BI) biosynthesized Zn-doped-Cu NPs and (BII) plant extract. (C) XRD pattern, (D) UV-Vis spectrum, and (E) EDS test for Zn-doped-Cu NPs

(101), (102), (110), (103), (200), (112), (201), (004), and (202). The following temperatures revealed the crystallinity of the products: 31.57°, 34.26°, 36.05°, 47.34°, 56.47°, 62.75°, 67.82°, 68.0°, 72.0°, 76.0°, and 81.0° [Figure 1C]. The FTIR method was employed to identify the chemical groups in the produced Zn-doped-Cu NPs. Figures 1BI and 1BII illustrate the spectra of the FTIR test for Zn-doped-Cu NPs and *U. dioica* extract, respectively. According to these spectra, bands appearing at 646 cm^{-1}, 1638 cm^{-1}, and 3453 cm^{-1} correspond to the O-H bond, C═C double bond, and O-H overlap, and N-H stretching in the structure of the extract, respectively. Additionally, sharp and prominent peaks within the 518, 1359, 1609, 2919, and 3431 cm^{-1} are observed in the FTIR spectrum of Zn-doped-Cu NPs. The FTIR spectrum reveals typical vibrations of copper oxide pigment at 518 cm^{-1}. Absorption peaks at 1609 and 2919 cm^{-1} are likely attributed to the carbonyl C = O group and the aldehyde stretching of the C-H bond, respectively. The pronounced peak in the 3431 cm^{-1} region indicates a significant amount of hydroxyl (OH) groups in the structure.

Cytotoxicity of Zn-doped-Cu NPs against MDA-MB-231 cell lines and MCF10A

The cytotoxicity of the *U. dioica* extract and biosynthesized Zn-doped-Cu NPs on BC cells (MDA-MB-231) was evaluated using the MTT assay. This assay determined the viability of tumor cells across various concentrations of Zn-doped-Cu NPs and extract. As depicted in Figure 2, Zn-doped-Cu NPs reduced the viability of both MDA-MB-231 and MCF10A cells in a dose-dependent manner, with IC50 values of 310.24 µg/mL for the extract and 10.26 µg/mL for biosynthesized NPs, and respective values of 996.52 µg/mL and 1606.57 µg/mL for normal cells. Zn-doped-Cu NPs exhibited escalating cytotoxicity in a dose-dependent fashion, achieving maximum inhibition at 100 µg/mL (90% inhibition) of MDA-MB-231 cells. Treatment of MDA-MB-231 cells with concentrations ranging from 6.125 to 100 µg/mL for 24 hours resulted in a significant dose-dependent reduction in cell viability, indicating the cytotoxic effects of Zn-doped-Cu NPs. Conversely, lower doses of the plant extract did not exhibit cytotoxic effects on MDA-MB-231 cell viability, showing a significant reduction in cancer cell survival only at 50 µg/mL ($P < 0.05$) and 100 µg/mL ($P < 0.01$). Comparison between NP-treated and extract-only-treated cells revealed higher viability in NP-treated cells, while cells co-treated with NPs and extract also demonstrated significant viability compared to the control group.

The expression of apoptotic and metastatic genes

The role of biosynthesized Zn-doped-Cu NPs and *U. dioica* extract in activating the apoptotic pathway in BC cells was investigated using apoptotic and metastatic genes [Figure 3]. Based on Figure 3, it can be concluded that the plant extract does not induce significant alterations in the expression of the evaluated genes (*Bax*, *Bcl2*, *MMP2*, and *MMP9*). However, the IC50 concentration of Zn-doped-Cu NPs significantly increased the expression of *Bax* ($P < 0.001$) and decreased the expression of *Bcl2* ($P < 0.01$), *MMP2* ($P < 0.01$), and *MMP9* ($P < 0.001$) genes, indicating their involvement in apoptosis induction and metastasis prevention.

Cytotoxic and apoptotic assay using LDH and caspase 3 activity

Membrane damage caused by lactate dehydrogenase (LDH) leakage and apoptotic action measured by caspase 3 activity were observed as cytotoxicity endpoints. LDH activity indicates cell lysis, which releases the enzyme into the extracellular space during this process. A significant increase (almost double) in LDH activity was observed in cancerous cell lines after exposure to the biosynthesized NPs compared to MDA-MB-231 cells treated with the extract ($P < 0.001$) and the control group [Figure 4]. Upon treatment with *U. dioica* extract and Zn-doped-Cu NPs, caspase-3 was activated [Figure 5], a crucial event in the apoptotic pathway. In MDA-MB-231 cancer cells, caspase 3 activity increased when cells were treated with the IC50 concentration of both substances ($P < 0.05$ for plant extract and $P < 0.001$ for Cu-Zn NPs) compared to control cells. However, this increase in cells treated with NPs was almost twice the activity observed in cancer cells treated with the plant extract.

ROS overproduction in treated cancerous cells

Excessive increase in ROS levels indicates apoptosis induction in cells. Figure 6 demonstrates ROS production in MDA-MB-231 cells receiving the IC_{50} concentration of Zn-doped-Cu NPs and the extract compared to untreated cells ($P < 0.05$ for plant extract and $P < 0.001$ for NPs), suggesting that both

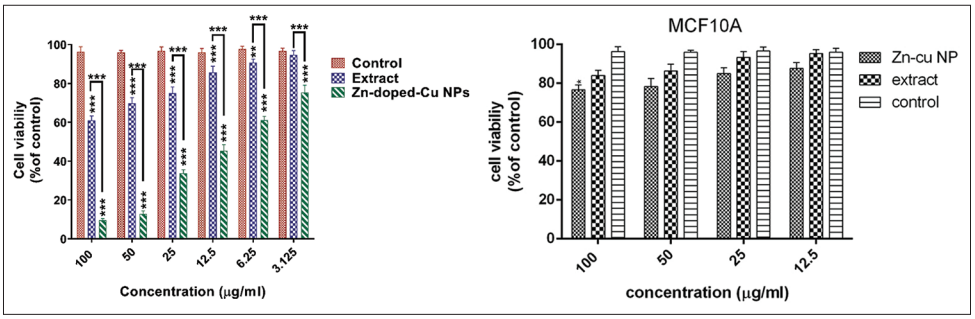

Figure 2: MTT assay for the viability of MDA-MB-231 cancer cells and MCF10A following treatment with different concentrations of biosynthesized Zn-doped-Cu NPs and *U. dioica* extract. Data are represented as mean ± SD, n = 3; **: *P <0.01* and ***: *P <0.001*

anti-cancer agents can elevate ROS levels in the BC cell line. Finally, the graphical abstract of the current study is shown in Figure 7.

Discussion

Bi-metallic NPs that have undergone bio-reduction are renowned for their non-toxic nature and valuable properties. They play a crucial role in medical research due to enhanced performance and reactivity driven by their quantum properties and the higher surface-to-volume ratio.[31] The study investigated the efficiency and environmental suitability of utilizing Zn-doped-Cu NPs synthesized using *U. dioica* against human MDA-MB-231 BC cells.

Characterization techniques, including UV-vis, FTIR, XRD, and EDX analyses, confirmed the presence of various secondary metabolites from the extract on the surface of doped NPs. Specifically, flavonoids, amides, aromatic compounds, and amino acids in the *U. dioica* extract acted as bio-reducing agents, converting Zn^{+} and Cu^{+} ions into ZnNPs and CuNPs, respectively.[32] Incorporation of these substances onto NP surfaces may enhance the efficacy of Zn-doped-Cu NPs as apoptotic therapies through synergistic effects.

Demonstrated that the cytotoxicity of bio-synthesized NPs at lower doses against cancer cells was significantly higher than that of the extract-treated group. Due to oxidative stress and lipid peroxidation, cells exposed to nanomaterials are more susceptible to membrane disruption, DNA damage, and eventual cell death. These NPs generate ROS by accepting electrons and interacting with H_2O_2 molecules in the cellular environment.[33] Green-synthesized copper NPs using *Prunus nepalensis* phytochemicals exhibited anti-cancer potential in BC cells (MCF7). The IC_{50} values of *Rheum rhaponticum*-synthesized ZnO-NPs against MCF-7 at 72, 48, and 24 hours

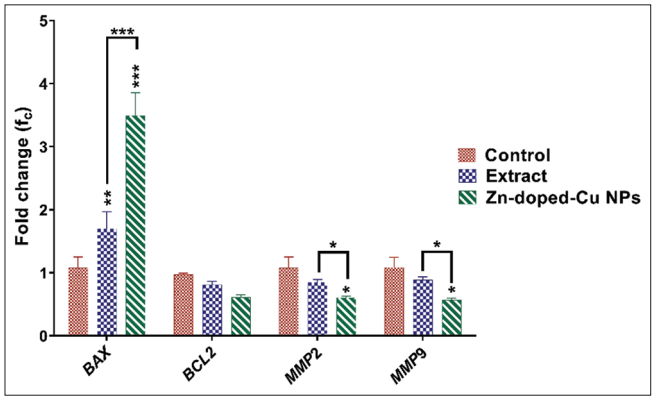

Figure 3: Real-time PCR assessment for *Bax*, *Bcl2*, *MMP2*, and *MMP9* expression in MDA-MB-231 cancer cells following treatment with the IC50 concentration of biosynthesized Zn-doped-Cu NPs and *U. dioica* extract. Data are represented as mean ± SD, n = 3; *: *P <0.05*, **: *P <0.01*, and ***: *P <0.001*

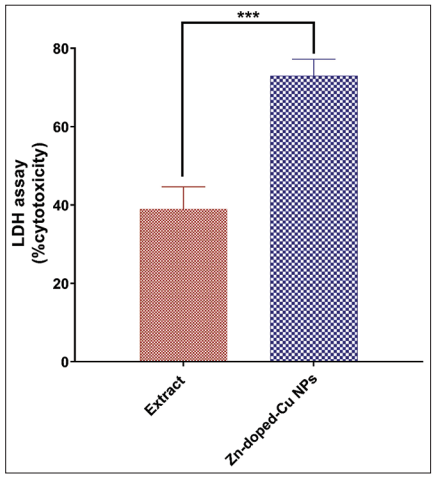

Figure 4: Comparison of LDH enzyme activity in MDA-MB-231 cancer cells following treatment with the IC_{50} concentration of biosynthesized Zn-doped-Cu NPs and *U. dioica* extract compared to the control group. Data are represented as mean ± SD, n = 3; ***: *P <0.001*

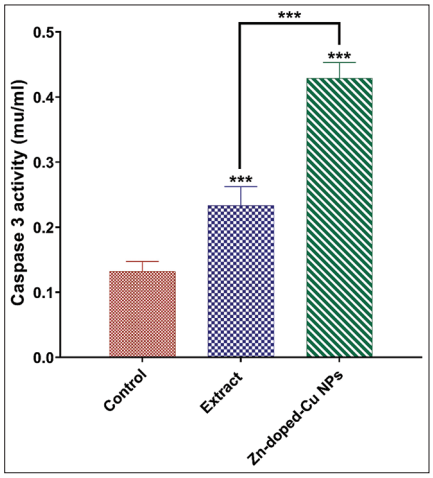

Figure 5: Comparison of Caspase-3 enzyme activity in MDA-MB-231 cancer cells following treatment with the IC_{50} concentration of biosynthesized Zn-doped-Cu NPs and *U. dioica* extract compared to the control group. Data are represented as mean ± SD, n = 3; ***: *P <0.001*

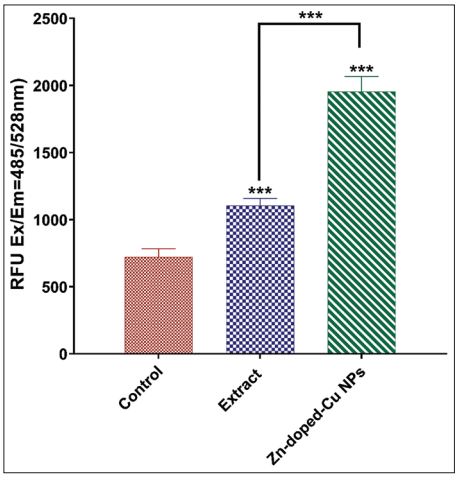

Figure 6: Comparison of ROS generation in MDA-MB-231 cancer cells following treatment with the IC50 concentration of biosynthesized Zn-doped-Cu NPs and *U. dioica* extract compared to the control group. Data are represented as mean ± SD, n = 3; ***: *P <0.001*

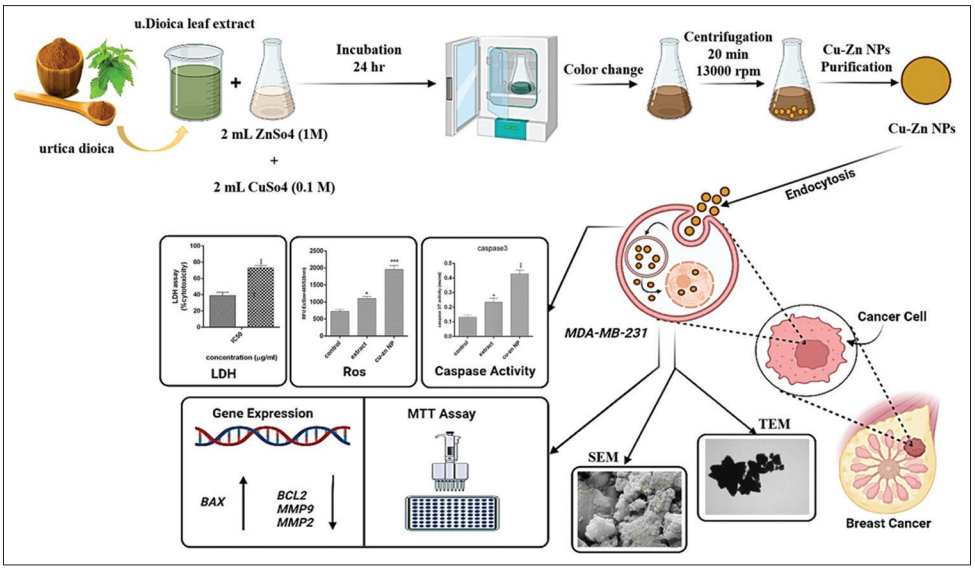

Figure 7: The study design as a graphical abstract

were assessed as 8, 11, and 12 µg/mL, respectively, which were comparable to those findings.[34] Pouresmaeili *et al*.'s study indicated that the IC_{50} values of green-synthesized ZnO-NPs using carob extracts at 24, 48, and 72 hours were 125, 62.5, and 31.2 µg/mL, respectively. Another study reported the IC_{50} of *Prunus nepalensis*-mediated CuNPs as 158.5 µg/mL against the MCF-7 cell line.[35,36] These data collectively suggest the significant anti-cancer potential of the prepared NPs in the investigation due to the combined activity of CuO NPs and ZnO NPs against human BC cells.

Various mechanisms are associated with inhibiting growth and cytotoxic effects of cancer cells by Zn-Cu NPs. These NPs can produce ROS in cancer cells by disrupting the electron transport chain in mitochondria and the Fenton reaction. ROS generation results in oxidative stress, causing damage to DNA and other cellular components, ultimately leading to cell death. Zn-Cu NPs can also physically interact with the cell membrane of cancer cells, causing damage and increased permeability, disrupting the cell's internal environment, and triggering apoptosis. Furthermore, Zn-Cu NPs can interfere with signaling pathways involved in cell proliferation and growth, leading to cell cycle arrest and inhibition of cancer cell division and multiplication.

Additionally, they may possess anti-angiogenic properties, inhibiting the formation of new blood vessels necessary for tumor growth and survival. Some studies suggest that Zn-Cu NPs can modulate the immune system, potentially enhancing the body's anti-tumor immune response and contributing to their anti-cancer effects. It is essential to note that the specific mechanism of action of Zn-Cu NPs on cancer cells may vary depending on nanoparticle size, shape, surface charge, composition, and the type of cancer cell targeted. Further research is necessary to fully comprehend the complex mechanisms involved and optimize using Zn-Cu NPs for cancer therapy. Research on the application of Zn-Cu NPs for cancer treatment is still in its early stages, and additional clinical trials are required to evaluate their safety and efficacy. Potential side effects of Zn-Cu NPs, including genotoxicity and cytotoxicity, need careful consideration before their use in humans. Combination therapy with other cancer treatments may be necessary to enhance the effectiveness of Zn-Cu NPs.[37-41]

Reactive oxygen species (ROS) are naturally produced by cellular processes such as respiration. At low levels, they act as signaling molecules in various pathways. However, excessive ROS generation leads to oxidative stress, damaging DNA, proteins, and lipids. This oxidative stress can induce cancer cell death through apoptosis and necrosis. ROS can promote cancer cell proliferation and survival in moderate amounts by activating pathways involved in growth and migration. This underscores the complex and context-dependent role of ROS in cancer. Catalase is a crucial enzyme for mitigating oxidative stress by efficiently decomposing hydrogen peroxide (H_2O_2), a major ROS species, into water and oxygen. Cancer cells often exhibit dysregulated antioxidant mechanisms, including elevated catalase activity, to counter their inherently higher ROS levels and sustain their survival and growth. External stimuli or nanoparticle exposure leading to higher ROS levels can overwhelm even elevated catalase activity, resulting in cytotoxicity and growth inhibition in cancer cells. Overexpression of catalase and other antioxidant enzymes can contribute to cancer cell resistance to ROS-generating therapies.

Targeting catalase or other antioxidant pathways alongside ROS-inducing treatments could be a promising strategy to overcome resistance. The relationship between ROS and catalase in cancer is dynamic and context-dependent. While catalase protects cancer cells from ROS-induced damage, it can also be exploited as a therapeutic target to enhance the efficacy of ROS-based cancer therapies. Further research is needed to

fully understand the intricate interplay between ROS, catalase, and other antioxidant systems in different cancer types and develop personalized therapeutic strategies. The information provided here offers a general overview, and specific details may vary depending on the type of cancer, treatment utilized, and other factors. I am not a medical professional, so I cannot provide medical advice. Please consult a qualified healthcare provider for any questions or concerns regarding cancer treatment.[40,42,43]

The mitochondria-associated apoptosis pathway was induced by altering the ratio of these *Bcl-2 protein* family members, upregulating proapoptotic *Bax*, and downregulating antiapoptotic *Bcl-xL* and *Bcl-2* expression.[30,34-46] Due to the altered activity of these proteins, ATP production is hampered by mitochondrial dysfunction.[45] The most significant up-regulation of the *Bax* gene (as a proapoptotic gene) and down-regulation of *Bcl2 (*as an antiapoptotic gene), *MMP2*, and *MMP2* (as a metastatic gene) was observed in MDA-MB-231 cells treated with *U. dioica*-mediated Zn-doped-Cu NPs, with the alteration of mentioned genes being remarkably higher than in extract-treated cells.

Some researchers propose that metallic NPs might interact with mitochondria, with effects potentially being particle-specific or influencing mitochondrial enzymes required for normal function, in addition to oxidative stress-induced mitochondrial damage and altering *Bcl-2 proteins*.[46] Thus, the results of an experiment using real-time PCR revealed a considerable overexpression of the genes *p53*, *caspase-3*, *Bax,* and *caspase-9* and a significant down-regulation of *Ras* and *Myc* mRNA expression in MCF-7 cells exposed to *Prunus nepalensis*-CuNPs.[36] Copper oxide NPs synthesized from green *Azadirachta indica* leaves trigger apoptosis by increasing *Bax* and caspase expression.[47] In other investigations, decreased mitochondrial membrane capacity due to Rehmanniae Radix-mediated ZnO-NPs activity caused elevated levels of apoptotic proteins, *caspase-3, caspase-9,* and *Bax,* leading to apoptosis in bone cancer MG-63 cells.[48] Extracts of Carob-mediated ZnO-NP-treated cells indicated that they could upregulate apoptosis and *Bax* expression and down-regulate Bcl-2 expression, inducing apoptosis in MCF-7 and MDA-MB231 cells.[49]

The fundamental role of matrix metallopeptidases, sometimes called matrix metalloproteinases (MMPs), which are zinc-associated proteolytic enzymes, is the breakdown and remodeling of extracellular matrix (ECM) constituents. The catalytic domain of MMP2 and MMP9 (gelatinases), belonging to separate classes of MMPs, comprises three fibronectin type II modules, which enhance substrate binding. Gelatinases can effectively break down collagen, gelatin, and elastin due to their structure but cannot hydrolyze small peptides.[50] The function of MMPs in the development and metastasis of malignancies is of special consideration. In nearly all forms of human malignancies, higher MMP expression and/or activity are highly correlated with a poorer prognosis, enhanced invasion, and the capacity to spread. MMPs are, therefore, potential therapeutic targets.[51] Accordingly, Au NP treatment reduced *MMP2* and *MMP9* expression and the quantity of the proteins they encode in squamous carcinoma SW579 cells.[52] A549 cell invasion and metastasis were shown to be inhibited by the phenylboronic acid-tagged ZnO NPs' ability to downregulate MMP-2 and VE-Cadherin.[53] Other studies demonstrated that CuO NPs reduced the survival of cancer cells, down-regulated *MMP-2* and *VEGF* expression, and induced apoptosis in 4T1 cancer cells.[54] Al Tamimi *et al*.[55] reported that treatment with Ag-Cu-NP in MCF-7 cell lines resulted in cytotoxicity and triggered a remarkable enhancement in MMP-9 levels, which contrasts with our study. This study indicated that Zn-doped-Cu NPs had significant apoptotic and antimetastatic activity against MDA-MB-231 cell lines through upregulating proapoptotic genes and down-regulating metastatic and antiapoptotic genes.

The findings revealed a higher increase in LDH and Caspase 3 enzyme activity in MDA-MB-231 cells after exposure to biosynthesized Zn-doped-Cu NPs, leading to a higher occurrence of apoptosis in cancer cells compared to the extract-treated group and control cells. The lactate dehydrogenase enzyme controls the lactate-pyruvate transition needed for cellular energy creation. When specific treated cells receive this enzyme in the culture media, the integrity of cell membranes is reduced. According to the findings, CuONPs should be able to improve LDH release independently. CuO NPs may enter BC cells and other biological elements, significantly degrading the cells and inducing the synthesis of LDH.[56] In malignant human skin melanoma cells, ZnO NPs caused lactate dehydrogenase leakage in a concentration- and time-dependent manner.[57] Based on research findings, CuNPs produced using Quisqualis indica extract may have caused cytotoxicity through a mechanism involving LDH release, ROS production, and GSH depletion in a dose-dependent manner.[58]

Quick and irreversible apoptosis is brought on by activated caspase-3, which can also cleave and activate additional caspase family members. Cell cycle checkpoint protein p53 causes cell cycle arrest when facing cellular stress or DNA damage to allow time for the loss to be fixed or for self-associated apoptosis.[59] ZnO NPs can activate the Caspase 3 protein in malignant human skin melanoma cells, according to research by Alarifi *et al*.[57] By inducing the production of Caspase 3, ZnO NPs from *Morus nigra* showed an anti-cancer effect in AGS (Human gastric carcinoma) cells. In human melanoma cells (A375), ZnO NPs derived from *Cardiospermum halicacabum* exhibit anti-cancer activities by upregulating the *Caspase 3* gene.[60] Previous data also indicate that CuONPs trigger up-regulation of *caspase-9* and *caspase-3* gene expressions and protein activity,[36,56,58,59] resulting in tumor cell death.

The elevation of ROS production in cells receiving Zn-doped-Cu NPs was approximately two-fold higher than the levels of ROS in cancer cells receiving plant extract. The outcomes support recent studies that identified increased ROS production

as the pivotal cytotoxic mechanism of green-synthesized Zn-doped-Cu NPs.[61,62] Enhanced production of ROS is significant for regulating the cell apoptosis process. A review study compiled data on CuONPs' anti-cancer activity, showing that green-synthesized CuONPs had great cytotoxic potential toward some colon cancer (HCT-116), BC (MCF-7, AMJ-13, and HBL-100 cells), cervical cancer (HeLa)[63], gastric cancer (human adenocarcinoma AGS cell line), leukemia cancer, lung cancer (A549), and other cancer types with the chief cytotoxicity procedure of elevating ROS generation. A large number of findings also indicate ROS production in cancerous cells after treatment with green-synthesized ZnONPs using *Alhagi maurorum* leaf (clone A141B1, G-292, MG-63, HOS, Hs 707(A).T, and Saos-2 cell lines),[64] Rehmanniae Radix (bone cancer cells MG-63),[48] Carob extract (MCF-7 and MDA-MB231 cells),[49] *Saponaria officinalis* (MCF-7 and MDA-MB231 cells),[35] *Morus nigra* (human gastric cancer AGS cell line),[65] Tea residue extracts (human lung cancer A549 cells A549).[66]

Conclusion

In this study, the rapid biosynthesis of Zn-doped-Cu NPs using *U. dioica* leaf extract, which proved to be a cost-effective and eco-friendly approach, has been demonstrated.

The biosynthesized Zn-doped-Cu NPs exhibited significant anti-cancer, antimetastatic, and antioxidant activity against the BC cell line. This was evidenced by cytotoxicity tests, alterations in proapoptotic and metastatic gene expressions, LDH and caspase-3 activity, and the over-production of ROS in MDA-MB-231 cells. The fabrication of Zn-doped-Cu NPs from *U. dioica* extract holds promise as a potential anti-cancer agent. Therefore, further *in vitro* and *in vivo* investigations are warranted to explore the application of Zn-doped-Cu NPs in targeting cancer cells within the human body.

Acknowledgments

The authors would like to acknowledge the Central Tehran Branch, Islamic Azad University, for providing the necessary laboratory facilities for this study.

Financial support and sponsorship

Nil.

Conflicts of interest

There are no conflicts of interest.

References

1. Consortium BCA. Breast cancer risk genes—association analysis in more than 113,000 women. N Engl J Med 2021;384:428-39.
2. Godone R, Leitão G, Araújo N, Castelletti C, Lima-Filho J, Martins D. Clinical and molecular aspects of breast cancer: Targets and therapies. Biomed Pharmacother 2018;106:14-34.
3. Pogorzelska A, Mazur M, Świtalska M, Wietrzyk J, Sigorski D, Fronczyk K, *et al*. Anticancer effect and safety of doxorubicin and nutraceutical sulforaphane liposomal formulation in triple-negative breast cancer (TNBC) animal model. Biomed Pharmacother 2023;161:114490.
4. Ruenraroengsak P, Kiryushko D, Theodorou IG, Klosowski MM, Taylor ER, Niriella T, *et al*. Frizzled-7-targeted delivery of zinc oxide nanoparticles to drug-resistant breast cancer cells. Nanoscale 2019;11:12858-70.
5. Brewer G, Hill G, Prasad A, Cossack Z. Biological roles of ionic zinc. Prog Clin Biol Res 1983;129:35-51.
6. Al-Saran N, Subash-Babu P, Al-Nouri DM, Alfawaz HA, Alshatwi AA. Zinc enhances CDKN2A, pRb1 expression and regulates functional apoptosis via upregulation of p53 and p21 expression in human breast cancer MCF-7 cell. Environ Toxicol Pharmacol 2016;47:19-27.
7. Chasapis C, Spiliopoulou C, Loutsidou A, Stefanidou M. The antioxidant properties of zinc. Arch Toxicol 2012;86:521-34.
8. Hanley C, Layne J, Punnoose A, Reddy K, Coombs I, Coombs A, *et al*. Preferential killing of cancer cells and activated human T cells using ZnO nanoparticles. Nanotechnology 2008;19:295103.
9. Alomari G, Al-Trad B, Hamdan S, Aljabali AA, Al Zoubi MS, Al-Batanyeh K, *et al*. Alleviation of diabetic nephropathy by zinc oxide nanoparticles in streptozotocin-induced type 1 diabetes in rats. IET Nanobiotechnol 2021;15:473-83.
10. Rajesh K, Umar A, Kumar G. Antimicrobial properties of ZnO nanomaterials. A review. Ceramics Int 2017;43:3940-61.
11. Agarwal H, Shanmugam V. A review on anti-inflammatory activity of green synthesized zinc oxide nanoparticle: Mechanism-based approach. Bioorg Chem 2020;94:103423.
12. Kaushik M, Niranjan R, Thangam R, Madhan B, Pandiyarasan V, Ramachandran C, *et al*. Investigations on the antimicrobial activity and wound healing potential of ZnO nanoparticles. Appl Surf Sci 2019;479:1169-77.
13. Mishra PK, Mishra H, Ekielski A, Talegaonkar S, Vaidya B. Zinc oxide nanoparticles: A promising nanomaterial for biomedical applications. Drug Discov Today 2017;22:1825-34.
14. Aljabali AA, Obeid MA, Bakshi HA, Alshaer W, Ennab RM, Al-Trad B, *et al*. Synthesis, characterization, and assessment of anti-cancer potential of ZnO nanoparticles in an *in vitro* model of breast cancer. Molecules 2022;27:1827.
15. Cao Y, Dhahad HA, El-Shorbagy M, Alijani HQ, Zakeri M, Heydari A, *et al*. Green synthesis of bimetallic ZnO–CuO nanoparticles and their cytotoxicity properties. Sci Rep 2021;11:23479.
16. Khalili P, Farahmandjou M. Nanofabrication of zinc ferrite (ZnFe2O4) composites for biomedical application. Chall Nano Micro Scale Sci Technol 2020;8:89-98.
17. Vickers NJ. Animal communication: When i'm calling you, will you answer too? Curr Biol 2017;27:R713-5.
18. Esposito S, Bianco A, Russo R, Di Maro A, Isernia C, Pedone PVJM. Therapeutic perspectives of molecules from Urtica dioica extracts for cancer treatment. Molecules 2019;24:2753.
19. Upreti S, Muduli K, Pradhan J, Elangovan S, Samant M. Identification of novel inhibitors from Urtica spp against MDAMB-231 targeting JAK 2 receptor for breast cancer therapy. Med Oncol 2023;40:326.
20. Soltani L, Darbemamieh M, Mohebi Z, Moarrefzadeh N. Comparison Of anti-cancer effects of hydroalcoholic extract of syzygium aromaticum and utrica dioica on breast cancer cells (Mcf-7) and normal cells (Huvec). Stud Med Sci 2021;32:175-86.
21. Karakol P, Saraydin SU, Bozkurt M, Hepokur C, Inan ZDS, Turan M. Anticancer effects of urtica dioica in breast cancer. Asian Pac J Cancer Prev 2022;23:673-81.
22. Nafeh G, Abi Akl M, Samarani J, Bahous R, Al Kari G, Younes M, *et al*. *Urtica dioica* leaf infusion enhances the sensitivity of triple-negative breast cancer cells to cisplatin treatment. Pharmaceuticals (Basel) 2023;16:780.
23. Aljabali AA, Akkam Y, Al Zoubi MS, Al-Batayneh KM, Al-Trad B, Abo Alrob O, *et al*. Synthesis of gold nanoparticles using leaf extract of Ziziphus zizyphus and their antimicrobial activity. Nanomaterials 2018;8:174.
24. Bangroo A, Malhotra A, Sharma U, Jain A, Kaur A. Biosynthesis of zinc oxide nanoparticles using catharanthus roseus leaves and their therapeutic response in breast cancer (MDA-MB-231) cells. Nutr Cancer 2022;74:1489-96.
25. Darvish M, Nasrabadi N, Fotovat F, Khosravi S, Khatami M, Jamali S, *et al*. Biosynthesis of Zn-doped CuFe 2 O 4 nanoparticles and their cytotoxic activity. Sci Rep 2022;12:9442.

26. Mahmood RI, Kadhim AA, Ibraheem S, Albukhaty S, Mohammed-Salih HS, Abbas RH, *et al*. Biosynthesis of copper oxide nanoparticles mediated annona muricata as cytotoxic and apoptosis inducer factor in breast cancer cell lines. Sci Rep 2022;12:16165.
27. Zhang H, Liu D, Wang L, Liu Z, Wu R, Janoniene A, *et al*. Microfluidic encapsulation of prickly Zinc-Doped copper oxide nanoparticles with VD1142 modified spermine acetalated dextran for efficient cancer therapy. Adv Healthc Mater 2017;6:1601406.
28. Afrand M, Sourinejad I, Fazeli SAS, Akbarzadeh A. Identification of engraulids (encrasicholina punctifer and E. pseudoheteroloba) using the COI gene as a DNA barcoding marker. J Aquat Ecol 2018;7:39-47.
29. Akhtar K, Khan SA, Khan SB, Asiri AM. Scanning electron microscopy: Principle and applications in nanomaterials characterization. Handbook of Materials Characterization. 2018. p. 113-45. Springer Cham https://doi.org/10.1007/978-3-319-92955-2.
30. Ramyadevi J, Jeyasubramanian K, Marikani A, Rajakumar G, Rahuman AA, Santhoshkumar T, *et al*. Copper nanoparticles synthesized by polyol process used to control hematophagous parasites. Parasitol Res 2011;109:1403-15.
31. Rasool S, Tayyeb A, Raza MA, Ashfaq H, Perveen S, Kanwal z, *et al*. Citrullus colocynthis-mediated green synthesis of silver nanoparticles and their antiproliferative action against breast cancer cells and bactericidal roles against human pathogens. Nanomaterials 2022;12:3781.
32. Botcha S, Prattipati SD. Callus extract mediated green synthesis of silver nanoparticles, their characterization and cytotoxicity evaluation against MDA-MB-231 and PC-3 cells. Bionanoscience 2020;10:11-22.
33. H N M. Synthesis of silver nanoparticles by using aloe vera and bio application. J Nanostructures 2023;13:59-65.
34. Salari S, Neamati A, Tabrizi MH, Seyedi SMR. Green-synthesized Zinc oxide nanoparticle, an efficient safe anticancer compound for human breast MCF7 cancer cells. Applied Organometallic Chemistry 2020;34:e5417.
35. Pouresmaeil V, Haghighi S, Raeisalsadati AS, Neamati A, Homayouni-Tabrizi M. The Anti-Breast Cancer Effects of Green-Synthesized Zinc Oxide Nanoparticles Using Carob Extracts. Anticancer Agents Med Chem 2021;21:316-326.
36. Biresaw SS, Taneja P. Copper nanoparticles green synthesis and characterization as anticancer potential in breast cancer cells (MCF7) derived from Prunus nepalensis phytochemicals. Mater Today Proc 2022;49:3501-9.
37. Aggarwal V, Tuli HS, Varol A, Thakral F, Yerer MB, Sak K, *et al*. Role of reactive oxygen species in cancer progression: Molecular mechanisms and recent advancements. Biomolecules 2019;9:735.
38. Dawane JS, Pandit VA. Understanding redox homeostasis and its role in cancer. J Clin Diagn Res 2012;6:1796-802.
39. Asaduzzaman Khan M, Tania M, Zhang DZ, Chen HC. Antioxidant enzymes and cancer. Chin J Cancer Res 2010;22:87-92.
40. Glorieux C, Calderon PB. Catalase, a remarkable enzyme: Targeting the oldest antioxidant enzyme to find a new cancer treatment approach. Biol Chem 2017;398:1095-108.
41. Preda C, Fulger L, Gheorghe L, Gheorghe C, Goldis A, Trifan A, *et al*. Adalimumab and Infliximab in Crohn's disease - real life data from a national retrospective cohort study. Curr Health Sci J 2016;42:115-24.
42. Ray PD, Huang BW, Tsuji Y. Reactive oxygen species (ROS) homeostasis and redox regulation in cellular signaling. Cell Signal 2012;24:981-90.
43. Nakamura H, Takada K. Reactive oxygen species in cancer: Current findings and future directions. Cancer Sci 2021;112:3945-52.
44. Pei J, Fu B, Jiang L, Sun T. Biosynthesis, characterization, and anticancer effect of plant-mediated silver nanoparticles using coptis chinensis. Int J Nanomed 2019;14:1969-78.
45. Gurunathan S, Qasim M, Park C, Yoo H, Kim J-H, Hong K. Cytotoxic potential and molecular pathway analysis of silver nanoparticles in human colon cancer cells HCT116. Int J Mol Sci 2018;19:2269. doi: 10.3390/ijms19082269.
46. Wang F, Chen Z, Wang Y, Ma C, Bi L, Song M, *et al*. Silver nanoparticles induce apoptosis in HepG2 cells through particle-specific effects on mitochondria. Environ Sci Technol 2022;56:5706-13.
47. Dey A, Manna S, Chattopadhyay S, Mondal D, Chattopadhyay D, Raj A, *et al*. Azadirachta indica leaves mediated green synthesized copper oxide nanoparticles induce apoptosis through activation of TNF-α and caspases signaling pathway against cancer cells. J Saudi Chem Soc 2019;23:222-38.
48. Cheng J, Wang X, Qiu L, Li Y, Marraiki N, Elgorban AM, *et al*. Green synthesized zinc oxide nanoparticles regulates the apoptotic expression in bone cancer cells MG-63 cells. J Photochem Photobiol B 2020;202:111644.
49. Pouresmaeil V, Haghighi S, Raeisalsadati AS, Neamati A, Homayouni-Tabrizi M. The anti-breast cancer effects of green-synthesized zinc oxide nanoparticles using carob extracts. Anti-cancer agents in medicinal chemistry (formerly current medicinal chemistry-anti-cancer agents). Anticancer Agents Med Chem 2021;21:316-26.
50. Matysiak-Kucharek M, Czajka M, Sawicki K, Kruszewski M, Kapka-Skrzypczak L. Effect of nanoparticles on the expression and activity of matrix metalloproteinases. Nanotechnol Rev 2018;7:541-53.
51. Galliera E, Tacchini L, Corsi Romanelli MM. Matrix metalloproteinases as biomarkers of disease: Updates and new insights. Clin Chem Lab Med (CCLM) 2015;53:349-55.
52. Zhang Q, Ma Y, Yang S, Xu B, Fei X. Small-sized gold nanoparticles inhibit the proliferation and invasion of SW579 cells. Mol Med Rep 2015;12:8313-9.
53. Mahalanobish S, Kundu M, Ghosh S, Das J, Sil PC. Fabrication of phenyl boronic acid mo1dified pH-responsive zinc oxide nanoparticles as targeted delivery of chrysin on human A549 cells. Toxicol Rep 2022;9:961-9.
54. Abbasi A, Ghorban K, Nojoomi F, Dadmanesh M. Smaller copper oxide nanoparticles have more biological effects versus breast cancer and nosocomial infections bacteria. Asian Pac J Cancer Prev 2021;22:893-902.
55. Al Tamimi S, Ashraf S, Abdulrehman T, Parray A, Mansour SA, Haik Y, *et al*. Synthesis and analysis of silver–copper alloy nanoparticles of different ratios manifest anticancer activity in breast cancer cells. Cancer Nanotechnol 2020;11:1-16.
56. Mahmood RI, Kadhim AA, Ibraheem S, Albukhaty S, Mohammed-Salih HS, Abbas RH, *et al*. Biosynthesis of copper oxide nanoparticles mediated annona muricata as cytotoxic and apoptosis inducer factor in breast cancer cell lines. Sci Rep 2022;12:16165.
57. Alarifi S, Ali D, Alkahtani S, Verma A, Ahamed M, Ahmed M, *et al*. Induction of oxidative stress, DNA damage, and apoptosis in a malignant human skin melanoma cell line after exposure to zinc oxide nanoparticles. Int J Nanomed 2013:983-93.
58. Mukhopadhyay R, Kazi J, Debnath MC. Synthesis and characterization of copper nanoparticles stabilized with Quisqualis indica extract: Evaluation of its cytotoxicity and apoptosis in B16F10 melanoma cells. Biomed Pharmacother 2018;97:1373-85.
59. Srinivasula SM, Fernandes-Alnemri T, Zangrilli J, Robertson N, Armstrong RC, Wang L, *et al*. The Ced-3/interleukin 1β converting enzyme-like homolog Mch6 and the lamin-cleaving enzyme Mch2α are substrates for the apoptotic mediator CPP32. J Biol Chem 1996;271:27099-106.
60. Duan X, Liao Y, Liu T, Yang H, Liu Y, Chen Y, *et al*. Zinc oxide nanoparticles synthesized from Cardiospermum halicacabum and its anticancer activity in human melanoma cells (A375) through the modulation of apoptosis pathway. J Photochem Photobiol B 2020;202:111718.
61. Al-Sheddi ES, Farshori NN, Al-Oqail MM, Al-Massarani SM, Saquib Q, Wahab R, *et al*. Anticancer potential of green synthesized silver nanoparticles using extract of Nepeta deflersiana against human cervical cancer cells (HeLA). Bioinorg Chem Appl 2018;2018:9390784.
62. Alizadeh SR, Ebrahimzadeh MA. O-Glycoside quercetin derivatives: Biological activities, mechanisms of action, and structure–activity relationship for drug design, a review. Phytother Res 2022;36:778-807.
63. Kalaiarasi A, Sankar R, Anusha C, Saravanan K, Aarthy K, Karthic S, *et al*. Copper oxide nanoparticles induce anticancer activity in A549 lung cancer cells by inhibition of histone deacetylase. Biotechnol Lett 2018;40:249-56.
64. Chinnathambi A, Alahmadi TA. Zinc nanoparticles green-synthesized by Alhagi maurorum leaf aqueous extract: Chemical characterization and cytotoxicity, antioxidant, and anti-osteosarcoma effects. Arab J Chem 2021;14:103083.

65. Tang Q, Xia H, Liang W, Huo X, Wei X. Synthesis and characterization of zinc oxide nanoparticles from Morus nigra and its anticancer activity of AGS gastric cancer cells. J Photochem Photobiol B 2020;202:111698.
66. Mathizhagan TE, Subramaniyan V, Renganathan S, Elavarasan V, Subramaniyan P, Vijayakumar S. Bio-mediated zinc oxide nanoparticles through tea residue: Ecosynthesis, characterizations, and biological efficiencies. Sustainability 2022;14:15572.